

# Structural Hardening Mechanisms of Lead-Cadmium-Bismuth-Silver Alloys for Battery Grids

Soukaina Saissi<sup>1,\*</sup>, Elmadani Saad<sup>1</sup>, Youssef Ait Yassine<sup>2</sup>

<sup>1</sup>Laboratory of Physicochemistry of Materials and Processes, Hassan 1 University, 26000 Settati, Morocco.

<sup>2</sup>Laboratory of Thermodynamics and energy, Ibn Zohr University, 80000 Agadir, Morocco.

\*corresponding author: [saissisoukaina90@gmail.com](mailto:saissisoukaina90@gmail.com)

Received: 18 Oct 2020; Received in revised form: 08 Dec 2020; Accepted: 15 Dec 2020; Available online: 21 Dec 2020

©2020 The Author(s). Published by Infogain Publication. This is an open access article under the CC BY license

(<https://creativecommons.org/licenses/by/4.0/>).

**Abstract**— The return of equilibrium of structure state of supersaturated solid solutions of lead-cadmium-Bismuth-silver alloys has been studied by different techniques: hardness, micro-hardness, microscopy and X-ray diffraction. Two structural states were considered: raw casting alloy and rehomogenized alloy. We studied alloys Pb2%Cd1%Bi and Pb3,2%Cd2%Bi to which we added the following concentrations by weight of silver to elaborate our alloys: 0,07% Ag, 0,15% Ag, 0, 2% Ag and 0,3% Ag. The explored temperatures are: 20°C and 80°C. Overall, the influence of silver resides in a slight increase in hardness. For the alloy Pb2%Cd3%Bi0,07%Ag, the microstructure is characterized by the formation of Ag<sub>3</sub>Cd<sub>8</sub> compound during solidification.

**Keywords**— aging, alloy, battery grids, hardness, overaging.

## I. INTRODUCTION

It is undeniable that the global energy landscape will evolve considerably in the coming years. The need for the energy consumption of humanity and the diversification of supply sources call for the rapid development of materials by making them more efficient in terms of mechanical and electrochemical properties. This is the case of the lead acid battery.

The lead accumulator is the oldest and most used accumulator for energy storage, it is a means having several applications in all automotive industries, it is a source of storage, recyclable, low cost and of great maturity. The choice of this accumulator therefore requires the development of grids characterized by a good resistance to corrosion and improved mechanical properties [1].

A systematic study of hardening mechanisms of Pb-Cd-Bi alloys was made by Saissi and al [2]. In this paper we will treat the influence of minor additives on silver on the ternary system Pb-Cd-Bi. Silver is by nature an element accompanying lead. The solubility of silver in the solid lead is very low.

Two studies were conducted on the Pb-Ag alloys. The first was conducted by Mao and al [3] who observed a large grain structure phase in an alloy with 0.02% by weight of Ag. A second phase (rich in silver) is observed in the Pb 0.09% Ag alloy which appears mainly inside the grain and along the grain boundaries. The second was made by Gulyaev and al [4]. He showed that the hardness increases with the concentration of silver. The structure of these alloys depends essentially on the silver content. For contents between 0.1% and 0.3% by weight of silver, the amount of eutectic is very low. The structure is similar to that of pure lead because silver from the eutectic liquid accumulates the first joints of the matrix grains boundaries.

The first studies concerning the action of silver on the mechanical properties of alloys for battery grids have been undertaken on the Lead-antimony alloys. Since 1941, Finck and Dorblatt [5] reflect the significant improvement in mechanical strength (hardness, breaking load) induced a silver addition.

Hilali and al. [6,7] have been studied in a systematic way the hardening process PbCdAg alloys. The corresponding hardeners phenomena are similar to those of PbCd alloys

whose aging is done in two concurrent reactions: a continuous precipitation and a discontinuous transformation. On the other hand, the over-aging occurs by a discontinuous magnification with precipitation of Cd phase from fine precipitates in the same phase. The effect of silver on the element hardening mechanisms PbCd alloys results in a slight increase in hardness.

In order to further improve the mechanical and electrochemical properties of PbCdBi alloys, we undertook the study of the influence of minor additions of silver on the hardening mechanisms of these alloys.

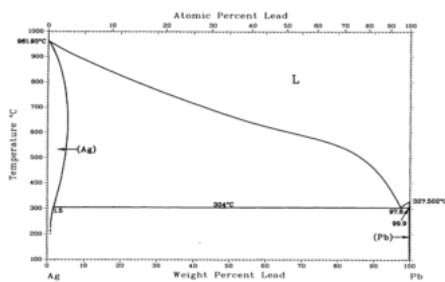
## II. MATERIALS AND METHODS

### 1.1. Preparation of alloys

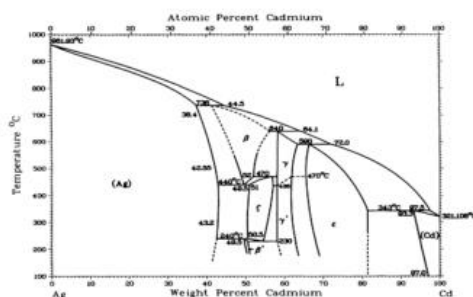
Pb-Ag binary system [8] has in the lead-rich side a much reduced solubility domain compared to that of the Pb-Cd systems. The system as shown in *fig.1a* has a eutectic at 304°C. The composition of the eutectic liquid is about 2.5 % by weight of silver. The solubility limit at the eutectic temperature is 0.1 % by weight of Ag.

Note that until now, there is no ternary diagram Pb-Cd-Ag or Pb-Bi-Ag in the literature. *Fig.1b* represents the phase diagram of Ag-Cd system [9]. According to the fields of Cd concentrations and temperature, more solid phases may be formed: (Ag),  $\beta$ ,  $\beta'$ ,  $\xi$ ,  $\gamma$ ,  $\gamma'$ , and  $\epsilon$  (Cd).

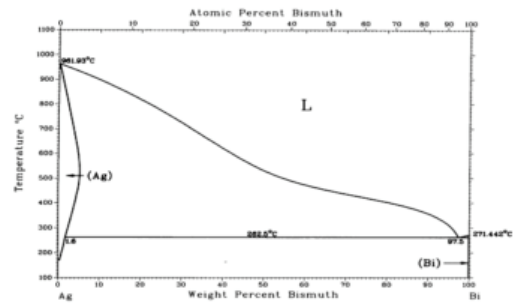
The binary system Bi-Ag [10] as is shown in *fig.1c* has a eutectic at 265.6°C. The composition of the eutectic liquid is about 2.5 % by weight of silver, while the maximum solubility of the bismuth in silver is 1.6 % by weight of silver.



a)



b)



c)

Fig. 1. a) Pb-Ag phase diagram b) Ag-Cd phase diagram  
c) Ag-Bi phase diagram

To study the structural-cast alloys, the elements taken in the proper proportions, are introduced into a silica ampoule of 8 mm in diameter, sealed under high vacuum, the mixture is heated to 500 °C. After melting and cooling total, the tube is quenched with water. The samples were examined directly or may be stored in liquid nitrogen. For rehomogenization, the ingot obtained is cut into several pieces that are then polished by abrasion. Samples are introduced into silica ampoules sealed under high vacuum. The whole is kept at 264 °C for 2 h (estimated optimal for rehomogenization) and then quenched with water [11,12].

### 1.2. Hardness:

The hardness tests are carried out by the Vickers method, using a durometer testwheel under a load of 2 kgf. Each measurement is the average of up to five trucks spread over a flat section corresponds to a diametric plane or perpendicular to the axis of the cylindrical sample.

The sections are obtained by sawing, mechanical abrasion and chemical polishing. Recall that the empirical relation  $HV = 0,3 (R)$  can be used to evaluate the rupture strength (R) of these alloys.

### 1.3. Technical micrographic observation

The physical properties of solid solutions for soaked lead alloys change from room temperature. The curing mechanisms correspond to continuous and/or discontinuous transformations. Indeed, this temperature corresponds to 0,5  $T_{\text{fusion}}$  (°K), temperature at which the alloy elements can diffuse. The observation of the structure of alloys corresponding to the continuous/discontinuous transformations is made by using the optical microscope, the samples must undergo mechanical polishing, chemical polishing using hydrogen peroxide 30%  $H_2O_2$  and three share of glacial acetic acid for 20 seconds to 2 minutes, then chemical attack using 100g of ammonium molybdate; 250 g of citric acid and water in sufficient quantity to have a liter of the mixture [13].

### III. RESULTS AND DISCUSSION

#### 3.1 Study of alloy Pb2%Cd1%Bi0,15% Ag:

##### 3.1.1 Hardness :

Fig.2 shows the change in hardness with time of the as cast alloy Pb2%Cd1%Bi 0,15% Ag at temperatures 20 °C and 80 °C. The initial hardness is of about 12,5 HV, it is much higher than that of pure lead (5 HV). This shows that partial conversion has already hardened the alloy during cooling. At room temperature, hardness increases to reach a value of about 13,233 HV after 8 hours. Then the hardness slightly decreased to reach 11,5 HV after 6 months.

At 80 ° C, the kinetics of transformation is more accelerated and the maximum hardness obtained is of about 13,27 HV. Beyond the 55 min, over-aging occurs and the hardness decreases significantly to peak 11 HV after 6 months.

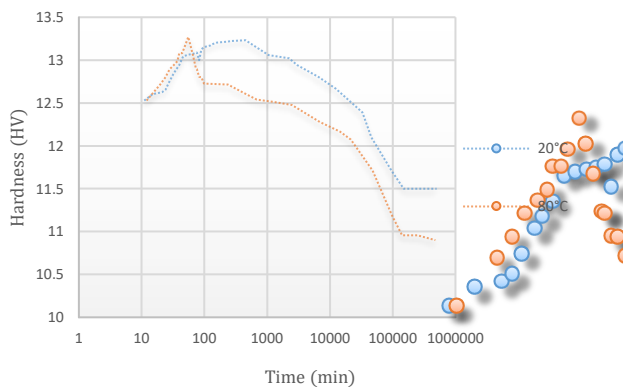


Fig.2. Evolution of hardness of the as-cast alloy Pb2% Cd1% Bi 0.15% Ag at temperatures 20°C and 80°C.

##### 3.1.2 Evolution of quenching structure :

The return to equilibrium of quenching structure was followed at various temperatures. Fig.3a and fig.3b show the discontinuous transformation of the alloy Pb2% Cd1% Bi 0.15% Ag. Indeed, aging is characterized by a continuous hardening reaction and softening discontinuous processing. The technique of chemical attacks repeatedly developed by Hilger [13, 14] allowed highlighting the fronts of the discontinuous reaction processing as shown in fig.3c and fig.3d.

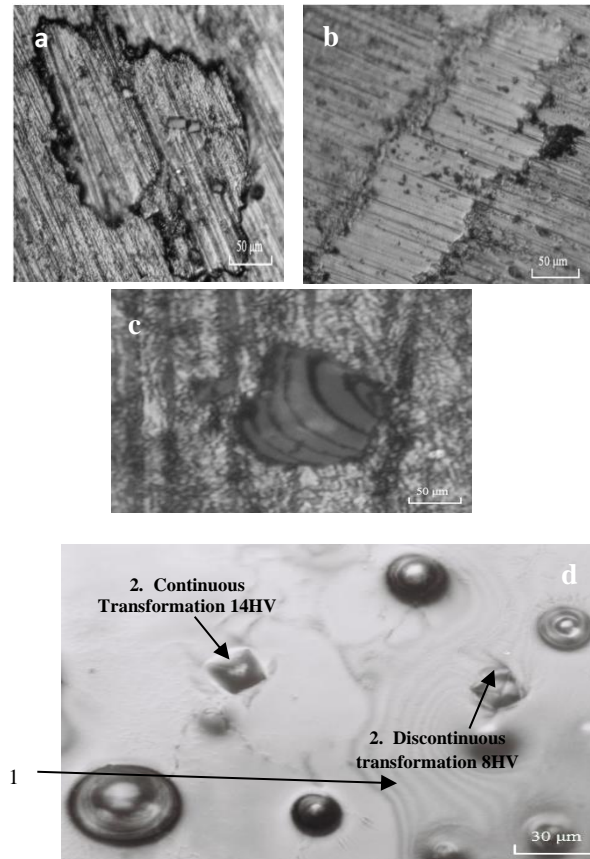
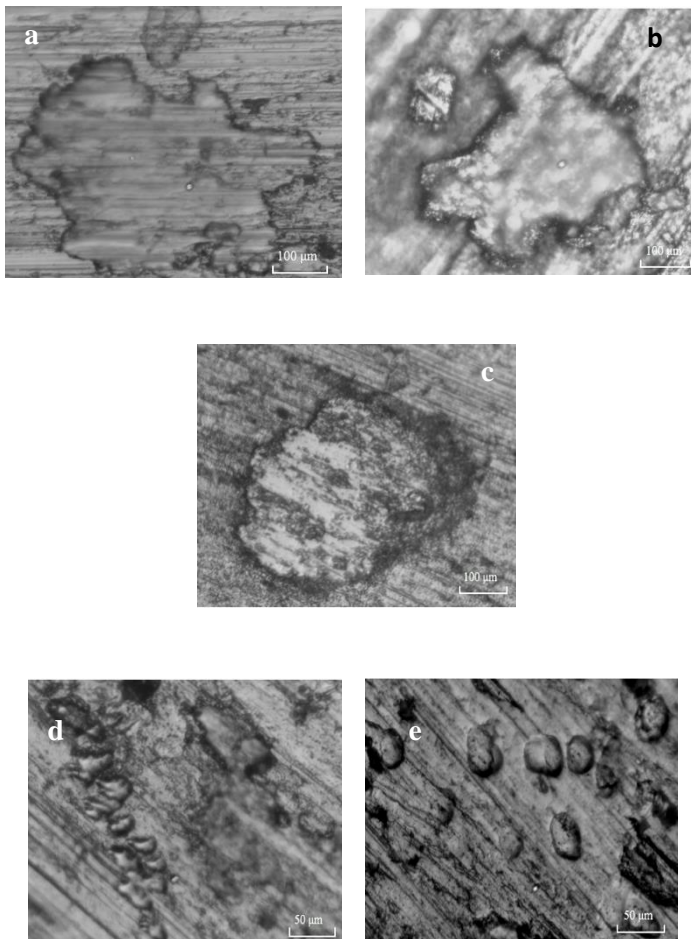


Fig.3. Evolution of quenching structure for as-cast alloy Pb2% Cd1% Bi 0.15% Ag. Visualization of the discontinuous transformation. a) Aging after 1 hour of quench. b) Aging after 3 hours of quench. c) after successive chemical attacks after quenching after 5 hours of quench. d) Visualization of 1. displacement of fronts transformations after successive chemical attacks 2. Micro hardness footprints performed after quenching after 4 hours during aging.

After 4 hours of quenching, we took microhardness measurements and we found that areas transformed by discontinuous reaction are less hard than unprocessed by this reaction, this shows that the metallographic observations and micro-hardness tests are in compliance with hardness measurements (Fig.3.d).

For maintaining at 80 °C, aging manifests by a curing which seems to be close to that maintained at 20 °C as it can be seen on the curves of hardness of fig.2., Fig.4.a and fig.4.b visualize discontinuous transformations of the alloy Pb2%Cd1%Bi0,15%Ag maintained at 80 ° C during aging and over-aging.

For stand prolonged at room temperature, the overaging occurs. From the curves of hardness (*Fig.2*), the overaging is usually accompanied by a softening starting after about 8 hours of maintenance at room temperature. For stand prolonged at room temperature, the overaging occurs. It is manifested by magnification of discontinuous reaction, progressing to almost complete covering the sample. The precipitates from both reactions characterizing the aging coalesce together to form large precipitates (*Fig.4.c*) after one month the matrix become swept by precipitates (*Fig.4.d* and *Fig.4.e*).



*Fig.4. Visualization of the discontinuous precipitation of the as-alloy Pb2% Cd1% Bi0, 15% Ag .*

1. Maintained at 80 °C a) After 1 month of quench during aging b) after 3 days of quench during overaging c) After 1 month of quench during overaging. 2. Maintained at 20°C d) and e) after 1 month of quench.

### 3.1.3. Kinetic study of the softening discontinuous precipitation which characterizes the overaging of the alloy Pb 2% Cd 1% Bi 0,15% Ag:

The kinetics of softening discontinuous precipitation of the alloy Pb2%Cd1%Bi 0,15%Ag that characterizes

overaging was jointly investigated by hardness measurements. The heat treatments were carried out at temperatures 20 °C and 80 °C for times varying from 7 hours to 6 months at 20°C and 55 min to 6 months at 80 °C. And those are applying the law of Johnson Mehl-Avrami and method of Burke [15].

*Fig.5.a* shows changes in the degree of advancement  $x$  of the transformation as a function of  $\ln(t)$  for different temperatures 20 °C and 80 °C. This gives sigmoid curves, elongated along the axis of time. Variations in the degree of advancement at temperatures 20 °C and 80 °C are deducted from the hardness measurements of the *fig.2* relating to overaging.

The degree of advancement  $x$  is calculated from the following relationship (1) :

$$x = \frac{Hv(t) - Hv(0)}{Hv(\infty) - Hv(0)} \quad (1)$$

With:

$Hv(t)$ : hardness at the time (t)

$Hv(0)$ : The initial hardness of the discontinuous precipitation.

$Hv(\infty)$ : Final hardness

*Fig.5.b* represents the variation of  $\text{LogLog} \left( \frac{1}{1-x} \right)$  as function of  $\text{Log}(t-\tau)$ .

The start times of this transformation are respectively 7 min and 55 minutes for the temperatures 20 °C and 80 °C. This figure shows that the points are placed on straight lines. The progress of this reaction is in conformity with Johnson and Mehl-Avrami equation [15].

*Table.1* provides the values of the exponent  $n$  calculated from the slope of the straight lines of *fig.5.b* and the rate constants  $k$  for the different temperatures. The value of  $n$  is close to 0,5 for both temperatures.

The apparent activation energy  $Q$  can be calculated from the variations of the coefficient  $k$  as a function of temperature. Indeed, in the case where it has an immediate saturation of the sites, the germination rate becomes zero and the speed of the front obeys to the equation (2):

$$K = k_0 \exp \left( -\frac{Q}{RT} \right) \quad (2)$$

It should be noted that this expression implicitly assumes that the total number of germs formed is independent of temperature. This expression achieves the value of the activation energy relative on the envisaged kinetic regime through the logarithmic linearized representation (3):

$$\text{Log} \frac{k_1}{k_2} = - \left( \frac{Q}{R} \right) \left( \frac{1}{T_1} - \frac{1}{T_2} \right) \quad (3)$$



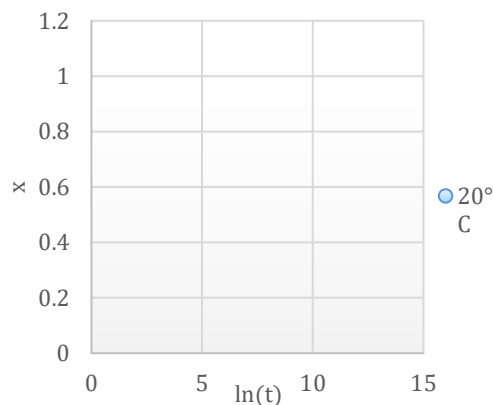
Assuming that  $k$  varies according to the Arrhenius law from the two coefficient values of Johnson and Mehl-Avrami equation relating to temperatures 20 °C and 80 °C characterizing the kinetics of the transformation during overaging in the case of the crude casting alloy Pb2% Cd1% Bi0,15% Ag quenched with water, the relationship (3) Gives an apparent activation energy  $Q$  associated with this reaction close to **12,075 KJ / mol**.

To verify that the activation energy does not depend on the degree of progress, we will use the method of Burke [15] which calculates activation energy without explaining the function which represents the experimental curves.

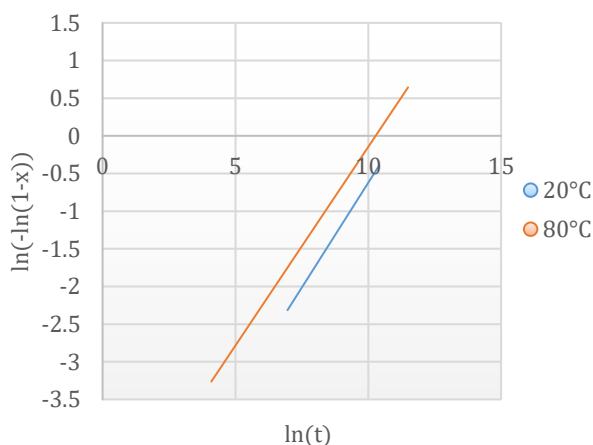
This method involves measuring the  $t_x$  time to reach a specified rate  $x$  of the precipitation. The  $\text{Log } t_x$  values are represented as a function of  $1/T$  in *fig.5.c* for various values of  $x$ .

The slope of these lines remains practically constant with  $x$  and determines an apparent activation energy  $Q$  with values reported in *Table.2*.

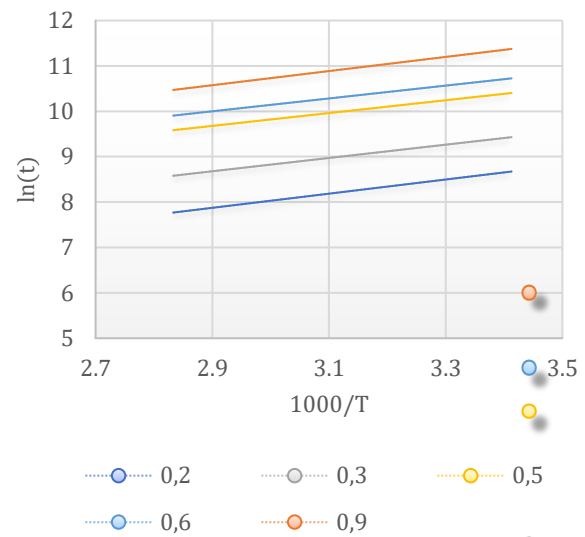
These values are close to the value of the activation energy **12,075 KJ / mole** given by the method of Burke [15].



(a)



(b)



(c)

*Fig.5. a) Alloy Pb 2% Cd 1% Bi 0, 15 % Ag. Transformed semi-logarithmic of curves from hardness tests at temperatures 20 ° C and 80 ° C on the softening discontinuous precipitation of crude casting alloy quenched with water. b) Representation  $\ln(-\ln(1-x))$  as a function of  $\ln(t)$  on the softening processing of overaging studied by isothermal hardness variations in the case of the crude casting alloy Pb 2% Cd 1% Bi 0,15% Ag. c) As-cast Alloy Pb2% Cd1% Bi 0,15% Ag. Variation of  $\text{Log } t_x$  as function of  $1/T$ .*

*Table.1. Coefficients of the equation of Johnson and Mehl-Avrami at different temperatures during overaging of the crude casting alloy Pb 2% Cd 1% Bi 0, 15 % Ag quenched with water.*

Temperature (°C)	n	k(s <sup>-1</sup> )
20	0,556	1,467.10 <sup>-5</sup>
80	0,527	3,402.10 <sup>-5</sup>

*Table.2. Values of the apparent activation energy  $Q$  for different processing rates in the case of as-cast alloy Pb2% Cd1% Bi 0,15% Ag quenched with water.*

Advancement degree x	Apparente activation energy $Q$ en (kJ/mol)
0,2	12,962
0,3	12,180
0,5	11,747
0,6	11,772
0,9	12,954

From **Table.2**, we found that the activation energy remains constant, it does not depend on the degree of advancement, and it is about **12,323 KJ / mol**. So we get a value that is about 8 times smaller than the energy of auto diffusion of lead which is of the order of 104,6 KJ / mol and the lowest compared to all the alloys studied in this report. This confirms the ease of the growth of the curing reaction.

### 3.2. Influence of silver

#### 3.2.1. Influence of silver on the alloy Pb2% Cd1% Bi

*Fig.6* shows the change in hardness with time of aging at room temperature for crude casting alloy Pb2% Cd1% Bi with contents by weight of silver: 0,07%, 0,15 % and 0,3%. Overall, these curves have almost the same pace as that of the raw casting alloy without silver [2]. Moreover, we note that the average of silver content (approximately 0,15%) which allows for maximum of hardness relatively high compared to other proportions.

Indeed, the influence of silver is translated as well: for low levels of silver, there is an increase in the maximum hardness and delay of the kinetics of transformations governing the hardening of these alloys. Gradually, as the silver concentration increases, the phenomena are reversed: we are witnessing a decrease in the maximum of hardness and an acceleration of the kinetics of hardening transformations.

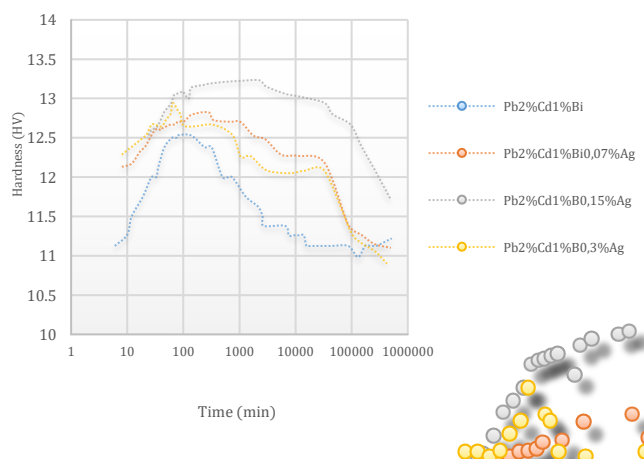


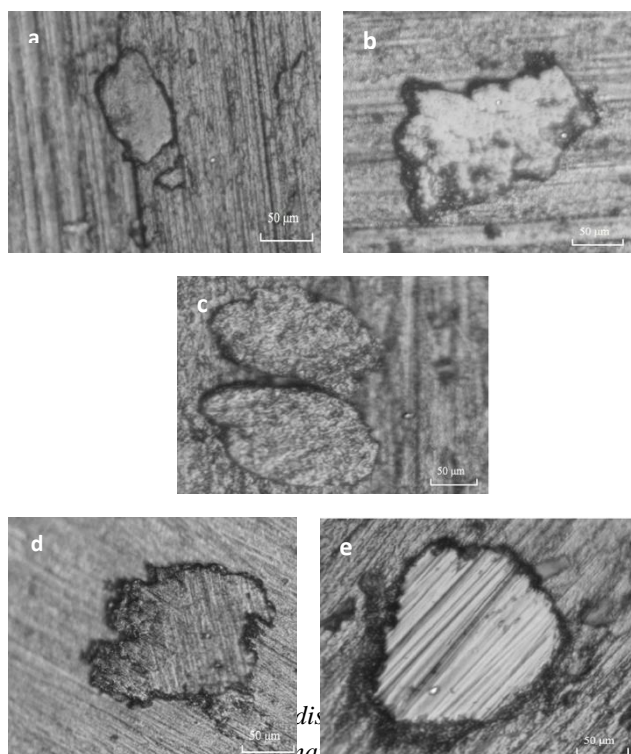
*Fig.6. Evolution of hardness as function of time at room temperature for the crude casting alloys Pb 2% Cd 1% Bi; Pb 2% Cd 1% Bi 0, 07 % Ag et Pb 2% Cd 1% Bi 0,15% Ag, Pb 2% Cd 1% Bi 0,3% Ag.*

#### 3.2.2. Evolution of quenching structure

Metallographic observations showed that the microstructures of the different raw casting alloys are the same. Indeed, we visualized the continuous and

discontinuous changes during aging and discontinuous precipitation during overaging in all studied alloys.

*Fig.7.a, fig.7.b and fig.7.c* show continuous and discontinuous changes in the alloy Pb 2% Cd 1% Bi 0,07% Ag during aging and overaging while *fig.7.d and fig.7.e* represent the transformations in the alloy Pb 2% Cd 1% Bi 0,3% Ag



*for Pb 2 % Cd 1 % Bi 0,07 % Ag . a) After 80 min of quench during aging b) After 1 day of quench during overaging c) after 2 days of quench during overaging. And for Pb 2% Cd 1% Bi 0,3% Ag d) After 50 min of quench during aging e) After 2 days of quench during overaging.*

#### 3.2.3. Influence of silver on the alloys Pb 2% Cd 3% Bi:

##### 3.2.3.1. Hardness

To see the influence of silver on the alloy that gave the strongest performance in terms of hardness we worked on the alloy strongly charged in Bismuth Pb 2% Cd 3% Bi.

*Fig.8* shows the change in hardness with time at temperature 20°C for the crude casting alloy Pb 2% Cd 3% Bi with different proportions on silver: 0.07 % Ag, 0.2 % Ag and 0.3 % Ag. Overall, these curves have almost the same pace in comparison with the influence of silver on the alloy lightly loaded on bismuth. The influence of high concentrations of silver results in a

retardation of the kinetics of transformation governing the structural hardening of these alloys and amplification of hardness. But more than the silver concentration increases the phenomena are reversed.

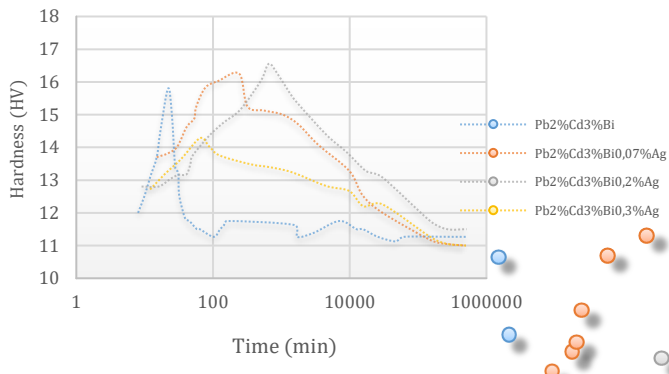


**Fig.8.** Evolution of hardness versus time at room temperature for as-cast alloys Pb 2 % Cd 3% Bi; Pb 2% Cd 3% Bi 0,07 % Ag, Pb 2 % Cd 3 % Bi 0,2 % Ag and Pb 2 % Cd 3 % Bi 0, 3 % Ag.

### 3.2.3.2. Evolution of quenching structure :

The evolution of quench structure was observed by optical microscopy at room temperature. We were able to see a grain boundary as shown in *Fig.9a*. We were also able to detect particular forms of precipitates due to the formation of a second phase during solidification of the alloy (*fig.9b* and *fig.9c*). For *fig.9b* and from the literature [5], it is the  $\text{Ag}_5\text{Cd}_8$  precipitate.

Indeed, analyzes by electron microprobe on the alloy Pb 3,2 % Cd 0,15 % Ag [5] shows that silver does not participate in hardening mechanisms of this alloy. It is almost completely contained in  $\text{Ag}_5\text{Cd}_8$  or congealed, in very small quantities in the grain boundaries. The influence of silver resides in a slight increase in the hardness of the quenched structure which is maintained over time. This increase is due to the presence of precipitates  $\text{Ag}_5\text{Cd}_8$  that are very hard.

In the alloy with 0,2 % Ag, is observed colonies precipitated as aureoles (or nodules) that probably

originate from the eutectic liquid (*Fig.10.a*). Gradually, as time increases we are seeing a growth of precipitate that scans the entire matrix (*Fig.10.b*).

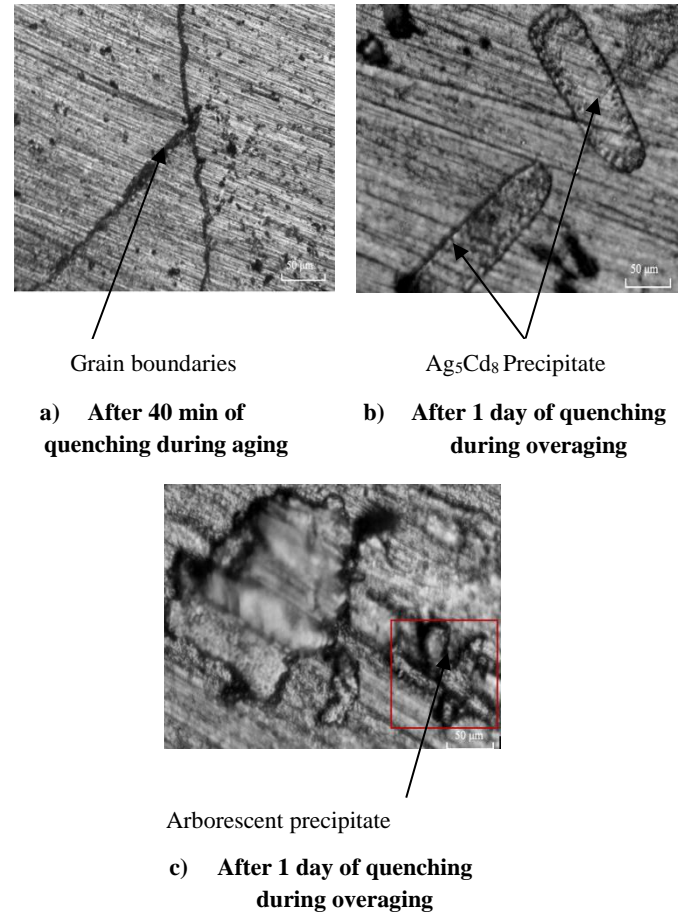


**Fig.9.** Visualization of a grain boundary of the as cast alloy Pb 2 % Cd 3% Bi 0,07 % Ag maintained at 20 °C during aging.

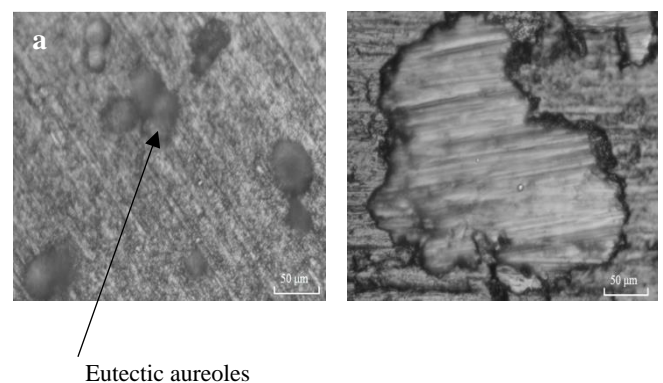


**Fig.10.** Visualisation of a) Eutectic mixtures of as-cast alloy of Pb2%Cd3%Bi0,2%Ag after 1 day of quenching maintained at 20°C during overaging b) Discontinuous precipitation of as-cast alloy Pb 2 % Cd 3% Bi 0,3 % Ag after 1 day of quenching maintained at 20°C during overaging.

By performing scanning electron microscopy (SEM) on the Pb 2 % Cd 3 % Bi 0.3 % Ag alloy after 1 year of aging (*Fig.11.a*), the energy-dispersive X-ray (EDX) analyzes

performed on the matrix (*Fig.11.b*) confirm the simultaneous presence of lead and bismuth with a very low proportion of cadmium. However, we did not detect silver (*Table.3*). This explains why the precipitate is rich in silver and cadmium, which is in conformity with the study of the structural hardening of the Pb-Cd-Ag alloy [6,7].

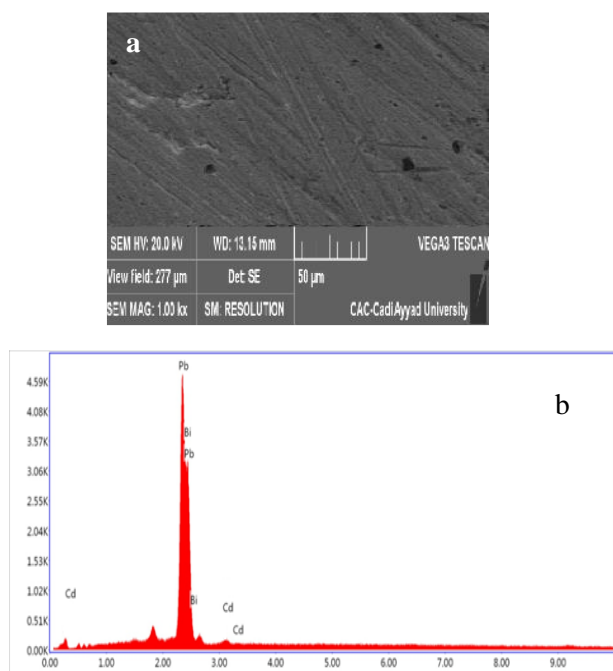


*Fig.11. Visualization by the a) SEM b) EDX of the matrix of the alloy Pb 2% Cd 3% Bi 0.3% Ag crude casting quenched with water at 20 ° C after 1 year of quenching.*

*Table.3. Results of the analyzes made by EDX carried out on the alloy Pb 2% Cd 3% Bi 0.3% Ag crude casting maintained after 1 year of quenching at room temperature.*

Analyzed phase by EDX	Element	Weight %
Matrix	Pb	80,21
	Bi	19,42
	Cd	0,37
	Ag	0
	Total	100

The X-ray diffraction (XRD) analysis performed on the alloy Pb 2% Cd 3% Bi 0,3% Mg only visualize the peaks of the solid solution  $\alpha$  lead, with a face centered cubic crystal structure.

However, we can't say that the precipitation of secondary phases has not occurred; the deduction we can make is that the XRD could not highlight such precipitation and this is because of the small size of the additive elements relative to that of lead.

*Fig.12* shows the results of XRD found on the alloy Pb 2% Cd 3 %Bi 0,3% Ag. While *table.4* bring together crystallographic parameters of these alloys.

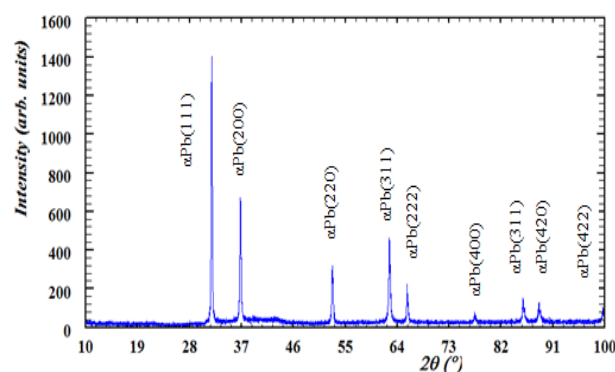


*Fig.12. X ray diffraction analyses of the surface of the alloy Pb 2% Cd 3% Bi 0,3% Mg.*

According to the X-rays diffraction pattern in *fig.12*, Treatment of diffraction patterns or spectra of the alloy Pb 2% Cd 3% Bi 0,3% Mg, highlights the peaks of the solid solution  $\alpha$  lead, with a crystalline structure CFC.

*Table.4. Crystallographic parameters of the alloy Pb 2% Cd 3% Bi 0,3% Mg.*

2θ [16]	2θ Calculated	d <sub>hkl</sub>	hkl	Parameter a (Å)
31.270	31.81890	2.81200	111	4.87052
36.262	36.71800	2.42963	200	4.85926
52.220	52.72969	1.72862	220	4.88927
62.139	62.64737	1.47371	311	4.88774
65.233	65.63463	1.40998	222	4.88431
76.985	77.34467	1.22942	400	4.91768
85.416	85.70898	1.12321	331	4.89595
88.189	88.45725	1.09134	420	4.88062
99.334	99.56984	1.00637	422	4.93018



### 3.3. Influence of rehomogenization treatment of the alloy Pb 2% Cd 1% Bi 0,15% Ag

#### 3.3.1. Hardness :

To study the influence of segregation cells of the solidification structure on mechanical properties, we conducted a parallel study on the rehomogenized alloy.

*Fig.13* shows the variations in hardness versus time of aging of the as-cast and rehomogenized alloys Pb 2% Cd 1% Bi 0,15% Ag kept at room temperature. We find that both alloys age in the same way but with an acceleration of the kinetics of the hardening process for the rehomogenized alloy. This acceleration is due to the dissolution of segregation cells from the solidification structure.

Indeed, the maximum hardness of the rehomogenized samples is 13,38 HV which is reached after 60 min while that of the as-cast sample is 13,23HV which is reached after 7 hours.

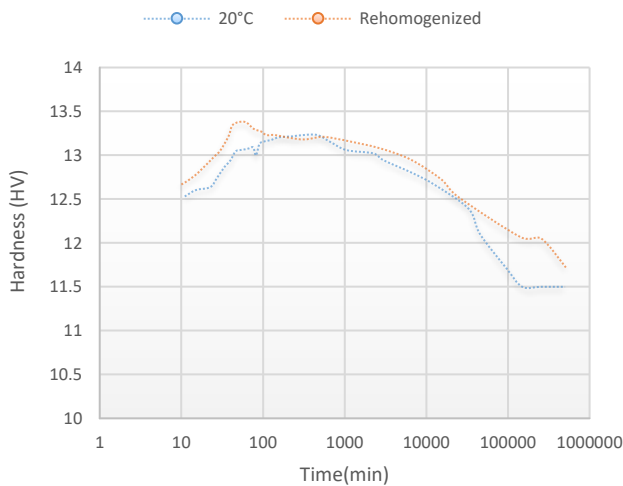


*Fig.13. Evolution of hardness versus time at room temperature for as-cast and rehomogenized alloy Pb 2% Cd 1% Bi 0,15% Ag.*

#### 3.3.2. Evolution of quenching structure

The micrograph of *fig.14.a* shows the initial structure of the rehomogenized alloy Pb 2% Cd 1% Bi 0,15% Ag, it is manifested by the presence of areas of eutectic mixtures. The early days of aging are characterized by the initiation of a discontinuous transformation (*Fig.14.b and 14.c*).

For prolonged maintain at room temperature, the *fig.14.d and fig.14.e* shows the areas processed by the discontinuous growth which is responsible for overaging, which is manifested by a discontinuous reaction mechanism.

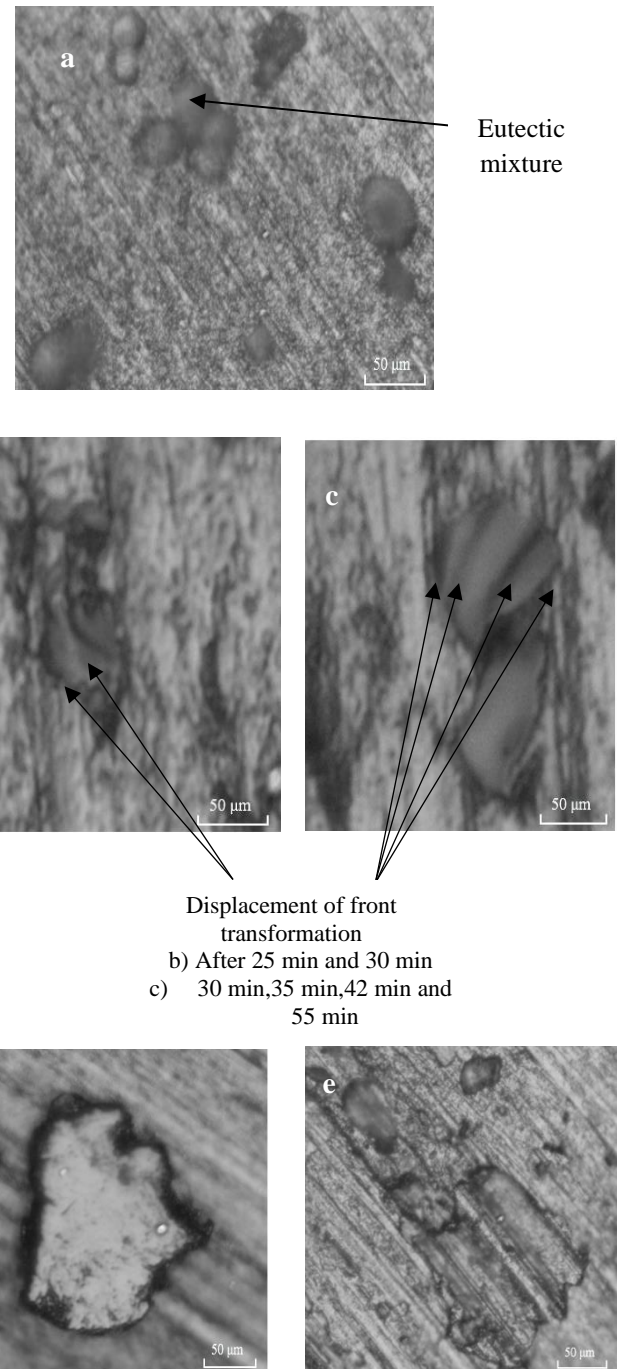


*Fig.14. Visualisation of rehomogenized alloy Pb 2% Cd 1% Bi 0,15% Ag maintained at 20°C a) eutectic mixtures after 20 min of quenching maintained at 20 ° C during aging. b) and c) Viewing the fronts of the discontinuous transformation after successive chemical attacks. d) Discontinuous precipitation after 1 hour of quench e) Discontinuous precipitation after 3 days of quench.*

#### IV. CONCLUSION

Several Researches has been done on lead alloys in order to improve mechanical and electrochemical properties, we cite Pb – Ca, Pb – Sb, Pb – Cd, Pb–Sr, Pb–Sn, Pb–Ca–Sn, Pb–Sb–Sn, Pb–Sb–Cd, Pb – Sr – Sn, etc.[17-30]

The phenomena of aging and overaging of PbCdBiAg alloys are similar to those of PbCdBi alloys. Indeed, the continuous and discontinuous transformations are the two concurrent reactions characterizing the aging. This discontinuous transformation is initiated by the displacement of the fronts of transformations. As against the over-aging is manifested by softening discontinuous precipitation.

The effect of silver on PbCdBi element alloys results in a slight increase in hardness. The presence of this element causes at time of solidification the formation of a particular microstructure. Indeed, we could visualize the  $\text{Ag}_5\text{Cd}_8$  compound which is formed during solidification of the alloy Pb 2% Cd 3% Bi 0,07% Ag.

The influence of high concentrations of silver results in a retardation of the kinetics of transformation governing structural hardening of these alloys and amplification of hardness. But more than the silver concentration increases the phenomena are reversed. Indeed, we find that it is the average contents of silver 0,15% Ag and 0,2% Ag that allow for relatively high hardness.

Aging mechanisms of rehomogenized alloys PbCdBiAg are similar to those of the crude casting alloys and we are witnessing an acceleration of the kinetics of the curing reaction. This acceleration is due to the dissolution of segregations cells from the solidification structure.

The X-ray diffraction analysis performed on alloys Pb 2% Cd 3% Bi 0,07% Ag and Pb 2% Cd 3% Bi 0,3% Mg only visualize the peaks of the solid solution  $\alpha$  lead, with a cubic face centered crystal structure, this is due to their small size. We also determined the parameters of the crystal structure of PbCdBiAg alloys.

Finally, a comparison of the hardness values obtained by alloys PbCdBiAg to those given by the ternary alloys PbCdBi shows the beneficial action of the additions of silver on the mechanical properties of these alloys.

#### REFERENCES

- [1] A. Kirchev, L. Serra, S. Dumenil, et al., "Carbon honeycomb grids for advanced lead-acid batteries. Part III: Technology scale-up," *J. Power Sources*, 299, 324 – 333 (2015).
- [2] S. SAISSI, K. MARBOUH, M. LAROUACH, Y. TAMRAOUI, E. SAAD, L. ZERROUK, B. MANOUN, Y. AIT YASSINE, L. BOUIRDEN, "structural hardening mechanism of Lead-cadmium-bismuth (tin-silver) alloys For battery grids", *Journal Of Science And Arts*, Year 14, No. 4(29), pp. 331-346, 2014.
- [3] G.W.MAO,J.G.LARSON,P.RAO, *Metallography*,(1969) pp 399,423.
- [4] GULYAEV,B.B., SINTER SPLAVOV, *Metallurgiya*, Moscow (1984) p 44.
- [5] C.G.Fink, A.J.Dornblatt, "The effect of silver (0,05% to 0,15%) on some properties and performance of antimonial lead storage battery grids", *Transactions of the Electrochemical Society*,79(1941) pp265-305.
- [6] E.Hilali, state thesis,"Etude des mécanismes de durcissement structural des alliages Pb-Cd,Pb-Cd-Sn, Pb-Cd-Ag, pour grilles de batteries". Ibn Zohr university, Agadir (1999).
- [7] E.Hilali, L.Bouirden, J.P. Hilger, "Structural hardening mechanisms of lead-cadmium-silver alloys for battery's grids", *Annales de chimie et sciences des matériaux*, 25 (1999) pp 91-100.
- [8] I.Karakaya, W.T.Thomson,1987 "alloys phase diagrams", Vol.3, ASM (1992) pp 258.
- [9] M. Hansen and K. Anderko "alloys phase Diagrams", vol 3, ASM (1992) pp 234.
- [10] R.P. Elliott and F.A. Shunk, 1980, "alloys phase Diagrams", vol 3 ASM (1992) pp 232.
- [11] E. Hilali, L. Bouirden, and J.-P. Hilger, "Structural hardening of lead-cadmium (tin-silver) alloys for battery's grids. I. Lead-cad- mium alloys," *Annales de Chimie, Science des Matériaux*, 24, 135 – 143 (1999).
- [12] E. Zantalla, Y. Ait Yassine, A. Aguzir, et al., "Structural hardening mechanisms of alloys PbCaSrAg for battery's grids," *J. Mater. Environ. Sci.*, 7, 2094 – 2105 (2016).
- [13] Hilger,J.P., "Métallographie du plomb et de ses alliages", cours de formation intensive de courte durée COMETT Nancy, textes rassemblés et édités par HilgerJ.P.: Laboratoire de thermodynamique Métallurgique, Université de Nancy I, N° ISBN: 29505658-2-0, pp 1-14.
- [14] J.P. Hilger, A.Boulahrouf, "Materials characterization", 24(1990),pp159-167.
- [15] Burke, "the kinetics of phases transformations in metals". Pergamon Press (1965).
- [16] Wyckoff R. W. G., "Second edition. Inter science Publishers, New York Cubic closest packed, ccp, structure", *Crystal Structures* 1(1963) 7-83.
- [17] J. Xiang, C. Hu, L. Chen, et al., "Enhanced performance of Zn(II)-doped lead-acid batteries with electrochemical active carbon in negative mass," *J. Power Sources*, 328, 8 – 14 (2016).
- [18] C. White, J. Deveau, and L. G. Swan, "Evolution of internal re- sistance during formation of flooded lead-acid batteries," *J. Power Sources*, 327, 160 – 170 (2016).
- [19] P.T.Moseley,D.A.J.Rand,andK.Peters,"Enhancingtheper- formance of lead-acid batteries with carbon – In pursuit of an understanding," *J. Power Sources*, 295, 268 – 274 (2015).
- [20] L. Yao, Y. Xi, G. Xi, and Y. Feng, "Synthesis of cobalt ferrite with enhanced magnetostriction properties by the sol-gel-hy- drothermal route using spent Li-ion battery," *J.*

*Alloys Comp.*, 680, 73 – 79 (2016).

- [21] M. Pino, D. Herranz, and J. Chacón, “Carbon treated commercial aluminum alloys as anodes for aluminum-air batteries in sodium chloride electrolyte,” *J. Power Sources*, 326, 296 – 302 (2016).
- [22] R. Ochoa, A. Flores, J. Torres, and J. Escobedo, “Manufacture of Al – Zn – Mg alloys using spent alkaline batteries and cans,” *Materials Today, Proc.*, 2, 4971 – 4977 (2015).
- [23] H. Gan, Y. Yang, and H. Shao, “Improvement of the rate performance of hydrogen storage alloys by heat treatments in Ar and H<sub>2</sub> GAr atmosphere for high-power nickel-metal hydride batteries,” *Electrochim. Acta*, 174, 164 – 171 (2015).
- [24] P. Wang, L. Shao, H. Yu, et al., “Observation on the electrochemical reactions of Li<sub>3-x</sub>Na<sub>x</sub>V<sub>2</sub>(PO<sub>4</sub>)<sub>3</sub> (0 ≤ x ≤ 3) as cathode materials for rechargeable batteries,” *J. Alloys Comp.*, 690, 31 – 41 (2017).
- [25] L.D.Trong, T.T.Thao and N.N.Dinh, “Characterization of the Li-ionic conductivity of La<sub>(2G3-x)</sub>Li<sub>3x</sub>TiO<sub>3</sub> ceramics used for all-solid-state batteries,” *Solid States Ionic*, 278, 228 – 232 (2015).
- [26] L. Bouirden, J. P. Hilger, and J. Hertz, “Discontinuous and continuous hardening processes in calcium and calcium-tin micro-alloyed lead: influence of ‘secondary-lead’ impurities,” *J. Power Sources*, 33, 27 – 50 (1991).
- [27] J. Hilger, “Déformation des alliages de plomb: compétition vieillissement – Recristallisation,” *J. Phys.*, IV, 05 (1995).
- [28] K. Takada, “Progress and prospective of solid-state lithium batteries,” *Acta Mater.*, 61, 759 – 770 (2013).
- [29] P.J.Hilger, “Hardening process in ternary lead-antimony-tin alloys for battery grids,” Proceedings of the Fourth European Lead Battery Conference, *J. Power Sources*, 53, 45 – 51 (1995).
- [30] R. Nozato, T. Yamaji, and H. Tsubakino, “Kinetics of Ag precipitation in a Pb – 0.038 at.% Ag alloy,” *Japan Inst. Metal*, 23, 500 – 504 (1982).